

Dynamic modelling of viral impact on cyanobacterial populations in shallow lakes: implications of burst size

Herman J. Gons*, Hans L. Hoogveld, Stefan G.H. Simis and Marjolijn Tjeldens

Netherlands Institute of Ecology (NIOO-KNAW), Centre for Limnology,
Rijksstraatweg 6, 3631 AC Nieuwersluis, The Netherlands.

*Corresponding author, e-mail: h.gons@nioo.knaw.nl

Laboratory experiments with whole water-columns from shallow, eutrophic lakes repeatedly showed collapse of the predominant filamentous cyanobacteria. The collapse could be due to viral activity, from the evidence of electron microscopy of infected cyanobacterial cells and observed dynamics of virus-like particles. Burst-size effects on single-host single-virus dynamics was modelled for nutrient-replete growth of the cyanobacteria and fixed viral decay rate in the water column. The model combined previously published equations for nutrient-replete cyanobacterial growth and virus–host relationship. According to the model results, burst sizes greater than 200 to 400 virions per cell would result in host extinction, whereas lower numbers would allow coexistence, and even stable population densities of host and virus. High-nutrient status of the host cells might accommodate a large burst size. The ecological implication could be that burst-size increase accompanying a transition from phosphorus to light-limited cyanobacterial growth might destabilize the virus–host interaction and result in the population collapse observed in the experiments.

INTRODUCTION

It has been well established that numerous viruses are associated with planktonic micro-organisms and significantly affect the population dynamics of their hosts (Wommack & Colwell, 2000; Suttle, 2005). The viruses of cyanobacteria, i.e. the cyanophages, were found to be ubiquitous in both inland waters and the marine environment (Suttle, 2000). Populations of free, infectious cyanophages show high turnover rates. Increases in cyanophage abundance by production of new phages is counteracted by loss processes, among which photodamage, adsorption onto host cells and other particles, and ingestion by protozoan grazers are important (Suttle & Chen, 1992). Although most experimental studies have been carried out on marine systems, there is little reason to doubt that the principles of cyanophage dynamics apply to natural aquatic environments in general.

Studies on *Synechocystis* and *Synechococcus* populations and associated cyanophages in coastal waters demonstrated that the phages imposed significant daily population losses, but presumably not the near-elimination of species (Suttle & Chan, 1993; Mühling et al., 2005). Although few studies provide adequate temporal resolution, coexistence of cyanobacteria and their phages appears to be the rule in inland waters. However, whole water-column experiments with natural lake water have indicated that the cyanobacterial population may collapse to virtual extinction under particular conditions of incident light and nutrient supply (Van Hannen et al., 1999; Gons et al., 2002). Such a collapse of the predominant plankton component drastically changes both the phototrophic and heterotrophic plankton communities (Van Hannen et al., 1999), and the concomitant increase in water transparency may promote

benthic production. Potential viral collapse of cyanobacterial populations therefore merits study of the causes and consequences, not only from the point of view of microbial ecology, but also because the phenomenon pertains to the whole food web.

In mathematical modelling, bacteria and bacteriophages have been considered as predator–prey associations showing oscillations in population densities as observed in many ecological studies. Levin et al. (1977) modelled such a predator–prey system for specific biota and habitat, i.e. *Escherichia coli* and its bacteriophage T2 in continuous cultures, and taking into account the prey growth in relation to resource availability. The model of Levin and co-workers was used later by Thingstad & Lignell (1997) and Bratbak et al. (1998), and served as a basis for the model described below. In eutrophic water bodies, the growth rate of phototrophic populations is continuously changing due to the population-density dependent mutual shading. An equation for light-limited cyanobacterial growth in whole water columns (Gons, 1995) replaced the coupling to the growth on glucose in Levin et al. (1977).

The present study aims to: (1) establish the parametrization of the model for the specific environment of well-mixed, shallow lakes; and (2) delineate potential destabilizing mechanisms in the cyanobacteria–cyanophage relationship in this environment. Results of modelling a single-host single-virus system without other biological interactions will be discussed. The problem will be addressed as to whether a lytic infection cycle may allow co-existence of dominant cyanobacteria with their phages as well as result in cyanobacterial population collapse. Regarding eutrophic water, nutrient-limited and light-limited growth may be alternating. Metabolic activity and nutrient status of the host cells are expected

Table 1. Model coefficients.

Symbol	Explanation	Value	Units
Cyanobacterial growth			
E_0	Downward irradiance at null depth	35	W m^{-2}
z	Water depth	2.0	m
μ^*	Maximum specific growth rate	0.5	d^{-1}
μ_c	Specific maintenance rate constant	0.03	d^{-1}
α_g	Initial slope of growth vs light	0.13	$\text{d}^{-1} (\text{W m}^{-2})^{-1}$
K_B	Background light attenuation coefficient	3.0	m^{-1}
k_c	Specific light attenuation coefficient	0.017	$\text{m}^2 (\text{mg Chla})^{-1}$
Cyanobacterium–cyanophage interaction			
c	Volume clearance rate per particle	0.014	$\mu\text{m}^3 \text{s}^{-1}$
σ_1	Fraction of virions adsorbed upon contact	1	
σ_2	Fraction of infective virions	1	
τ	Length of the lytic cycle	0.5	d
m	Burst size (virions released per cell)	50–1600	
γ	Virion specific decay rate	0.5	d^{-1}

Chla, chlorophyll-*a*.

to have marked effects on the assemblage of viral nucleic acids and proteins. These effects may be shown by length of the lytic cycle and the number of virions produced per cell, known as the burst size. Wilson et al. (1996) described effects of phosphorus-limited growth on both length of the lytic cycle and burst size of a cyanophage infecting cultures of the marine cyanobacterium *Synechocystis* sp. In experiments with the marine haptophyte *Phaeocystis pouchetii* infected by a lytic virus, the length of the lytic cycle appeared to be rather constant, but the burst size varied by more than a factor of 30 (Bratbak et al., 1998). Considering probability of infection of host cells, large burst-size variation merits particular attention in modelling host–virus relationships in plankton communities in general.

THEORY AND MODEL ENVIRONMENT

Symbols of model coefficients and their units are listed in Table 1. Considered here is light-limited growth of *Limnothrix* sp. from Lake Loosdrecht (The Netherlands), of which the trichomes in lake water were formerly identified as *Oscillatoria* cf. *limnetica*, a group of morphologically similar filamentous cyanobacteria (Van Tongeren et al., 1992; Zwart et al., 2005). For fully mixed water the specific growth rate can be related to depth-averaged light irradiance according to a saturation curve (Neale et al., 1991), adjusted for maintenance energy (Gons, 1995):

$$\mu = (\mu^* + \mu_c) \{1 - \exp[-\alpha_g E_a / (\mu^* + \mu_c)]\} - \mu_c \quad (1)$$

where μ =specific growth rate, μ^* =maximum of μ at the relevant temperature, μ_c =specific maintenance rate constant, α_g =initial slope of the saturation curve, E_a =depth-averaged downward irradiance. For optically deep water, E_a is approximately given by:

$$E_a = E_0 / (K_d z) \quad (2)$$

where E_0 =downward irradiance just below the water surface, K_d =attenuation coefficient for downward irradiance, z =water column depth. The value of K_d is a

function of the cyanobacterial population density, here given as chlorophyll-*a* (Chla) concentration:

$$K_d = k_c \text{Chla} + K_B \quad (3)$$

where k_c =Chla-specific attenuation coefficient for downward irradiance, K_B =background attenuation as determined by dissolved humic substances, detritus particles, and water. In the present simulations the value of K_B has been held constant.

Thus, the growth rate of a healthy population of cyanobacteria is obtained for specified incident light, water depth and background attenuation. If the cyanobacteria are associated with a virulent phage and no other population losses occur, the change in population density of healthy, uninfected cyanobacteria is given by (notation slightly modified from Bratbak et al., 1998):

$$dU/dt = \mu U - c\sigma_1\sigma_2 VU \quad (4)$$

where U =population density of uninfected cells, V =population density of free virions, c =host–virus contact rate expressed as a volume clearance rate per particle (see Murray & Jackson, 1992), σ_1 =fraction of virions adsorbed upon contact with host cell, σ_2 =fraction of infective virions. Cells are not only infected but also removed by their lysis when the lytic cycle is completed:

$$dI/dt = c\sigma_1\sigma_2 VU - c\sigma_1\sigma_2 V_{t-\tau} U_{t-\tau} \quad (5)$$

where I =population density of infected cells, τ =time between infection and release of virions by cell lysis. The dynamics of the free virions is determined by the number of virions released per lysed cell, their adsorption onto uninfected and infected cells, and their decay due to factors such as photodamage and ingestion by protists:

$$dV/dt = m c \sigma_1 \sigma_2 V_{t-\tau} U_{t-\tau} - c \sigma_1 V(U + I) - \gamma V \quad (6)$$

where m =virions released per cell, also known as burst size, γ =virion decay rate. In the present simulations the decay rate was held constant.

The model was programmed (STEM software, Remedy Systems Modelling, Enschede, The Netherlands) to simulate

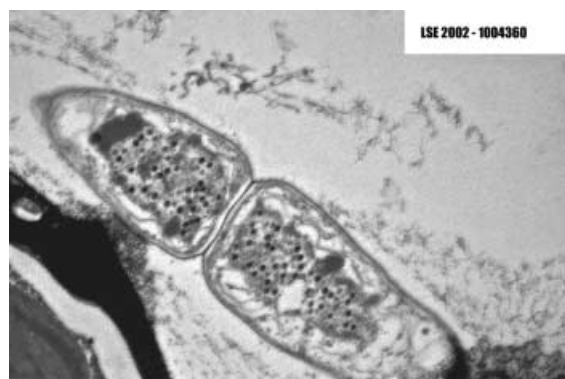


Figure 1. Transmission electron micrograph showing maturing virions with heads ~ 60 nm in diameter in thin section of cyanobacterial trichome from sample during population collapse in laboratory-scale enclosure of Lake Loosdrecht water (November–December 2002).

the population dynamics of the filamentous cyanobacterium *Limnothrix* sp. under nutrient-replete conditions in association with a hypothetical cyanophage in a 2-m deep, fully mixed water column at constant temperature of 20°C , receiving nutrient-rich medium at a dilution rate of 0.05 d^{-1} and continuous photosynthetically available radiation of 35 W m^{-2} ($160\text{ }\mu\text{E m}^{-2}\text{ s}^{-1}$) just below the water surface, and with $K_B=3\text{ m}^{-1}$. Except for the lack of a light–dark cycle, this physical environment corresponds to the laboratory-scale enclosure (LSE) of water from Lake Loosdrecht (The Netherlands), in which cyanobacterial mass lytic events had been observed (Van Hannen et al., 1999; Gons et al., 2002; Simis et al., 2005).

RESULTS

Model parametrization

Initial values of the model coefficients for nutrient-replete growth (Eqn 1, Table 1) were taken from Gons (1995). The values had been estimated from growth of *Limnothrix* sp. isolate MRI in the same laboratory-scale enclosures (Rijkeboer et al., 1993) as in which the observations were made on the cyanobacterial collapse in lake water. Additional parametrization was required for the cyanobacterium–cyanophage interaction.

In conditions of full mixing, the contact rate c is determined by the viral diffusivity and host cell size. In the course of mass lytic events, the filamentous cell arrangement in healthy *Limnothrix* sp. ultimately changes to random dispersal of single cells. The model does not account for effects on c by this morphological change of the host. Moreover, specific information on the values of the fractions σ_1 and σ_2 was lacking. For the present study, the observations on the mass lytic events in LSE (Gons et al., 2002; Simis et al., 2005) were used to calibrate a value of c —to be considered as an apparent contact rate, c^* —by setting the fractions σ_1 and σ_2 to 1. In real water columns these fractions may be small (Wommack & Colwell, 2000), thus the empirical c^* value is expected to be considerably lower than the contact rate computed from transport theory. If all virions were infective, the value of c^* equals the adsorption rate onto host cells.

The LSE experiments provided information about the remaining coefficients τ , m and γ . From the rapidity of the

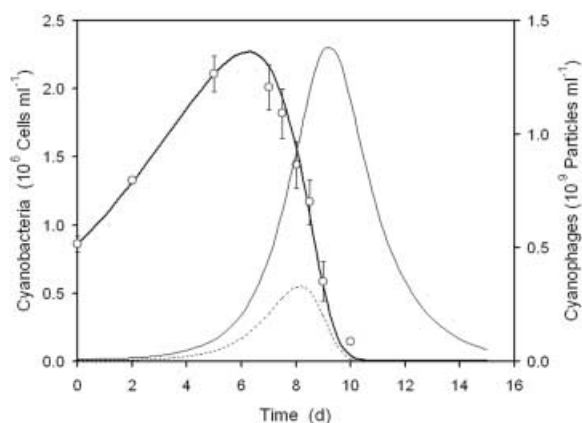


Figure 2. Model fit (thick solid line) for burst size of 900 virions per cell to averaged total cyanobacterial cell number (circles, with standard deviation bars) in three replicate laboratory-scale enclosures of Lake Loosdrecht water (March–April 2003); see Table 1 for other coefficients. Also represented are the modelled abundance of infected cyanobacterial cells (dotted line) and cyanophage abundance in suspension (thin solid line).

cyanobacterial collapse the length of the lytic cycle appeared to be <1 day, i.e. of similar duration as had been established for the cyanophage LPP-1 infecting freshwater filamentous cyanobacteria (Padan et al., 1970). By using transmission electron microscopy it was found that the burst size in LSE of Lake Loosdrecht water could amount to hundreds of virions per cyanobacterial cell (Figure 1), which also corresponds with observations on LPP-1 (Padan & Shilo, 1969a; Sherman & Haselkorn, 1971). The LSE experiments showed rapid decrease of the number of virus-like particles after cyanobacterial population collapse (Gons et al., 2002), indicating that the phage production was accompanied by a decay rate of about 0.5 d^{-1} . This value may be compared with the decay rates that have been estimated for various aquatic viruses, and are tabulated in Wommack & Colwell (2000).

Model calibration

Whereas estimates of the other parameters were available (Table 1), the model needed calibration for the apparent contact rate c^* . Model runs were made to fit a value of c^* for $m=900$, as estimated from electron microscopy (Figure 1), to cyanobacterial population dynamics in LSE (Figure 2). Because counts had been made of the trichomes but not of cells, the total cell numbers, i.e. the sum of healthy and infected cells, were calculated from the Chl *a* concentration, assuming a previously established number of 10^{10} cells per mg of Chl *a* in nutrient-replete conditions in LSE of Loosdrecht lake water.

Values of the state variables U , I , and V at time zero in the model were based on the Lake Loosdrecht water collected for the LSE experiments, in which the filamentous cyanobacterial population density of 5×10^5 to 10^6 cells ml^{-1} constituted $>99\%$ of the total number of phototrophic cells. It was assumed that the cyanobacteria were physiologically adapted to the LSE conditions after 2 d, which was taken as day zero for the modelling. In the course of cyanobacterial growth in LSE the algal share even decreased until the cyanobacterial mass lysis. The

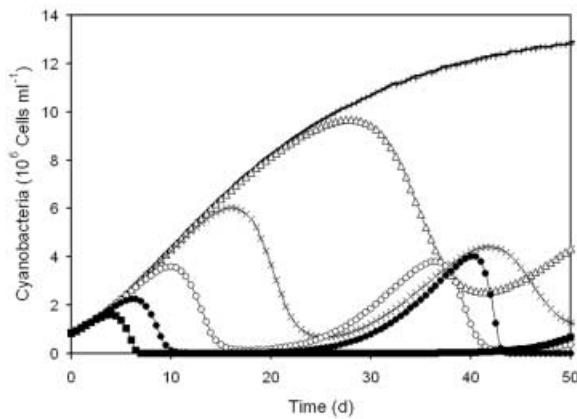


Figure 3. Modelled time course of population density of uninfected cyanobacterial cells depending on burst size (50, 100, 200, 400, 800 and 1600 virions per cell represented by thin lines with pluses, open triangles, crosses, open circles, solid dots and solid squares, respectively). Other coefficients as in Table 1. The thick solid line represents the cyanobacterial growth in the absence of viruses, thus solely depending on physical constraints.

initial population density of free virions associated with the filamentous cyanobacteria was assumed to be ten times that of the cells, and the share of infected cells was set at 1%. Whereas the simulations proved to be highly sensitive to variation in the values of both c^* and m , they were much less influenced by the numbers of U , I and V at time zero. Lowering the initial number of free viruses by a factor of 2 increased the maximum cyanobacterial population density by about 10%, while the time of the maximum was delayed only by half a day. Enhancement of the initial number of infected cells from 1% to 5% of the total population lowered the maximum population density by about 10%, and the population peak was reached half a day earlier than shown in Figure 2.

The values of α_g and k_c were adjusted by about 15% from their initial values (Gons, 1995) to better fit the curve to the maximum cell numbers, but their change did not significantly affect the value of c^* .

The value $c^*=0.014 \mu\text{m}^3 \text{s}^{-1}$ provided reasonable simulations of the cyanobacterial population growth and the timing of collapse in the LSE experiments (Figure 2). This value is one order of magnitude lower than the adsorption rate constant of 0.3 to $0.5 \mu\text{m}^3 \text{s}^{-1}$ reported for LPP-1 with a short-trichome mutant of *Plectonema boryanum* (Padan & Shilo, 1969b). The value is much smaller than 'true' contact rates in cultures of *Escherichia coli* and *Micromonas pusilla* tabulated in Murray & Jackson (1992), thus indicating that $\ll 1\%$ of the host–virus collisions would result in infection.

Burst size variation

Simulations for a wide range of burst sizes showed large, systematic effects of this parameter on cyanobacterial abundance in comparison to growth in absence of viruses (Figure 3). In the latter case, for the given combination of incident light, temperature and dilution rate in the LSE experiments, the population density would stabilize at 1.35×10^6 cells ml^{-1} , which corresponds to Chla and dry

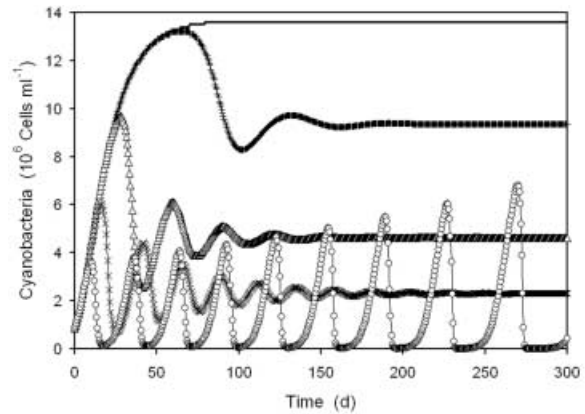


Figure 4. Modelled time course of cyanobacterial population density depending on burst size as in Figure 3, but with expanded time scale and leaving out the plots for burst sizes of 800 and 1600.

weight concentrations of 1350 mg m^{-3} and about 60 g m^{-3} , respectively, i.e. levels as obtained with cultured cyanobacteria in LSE (Rijkeboer et al., 1990). For $m=50$, there would be no significant effect of the virus on the cyanobacterial growth for nearly two months. For greater burst sizes the population density maxima would decrease from about two-thirds ($m=100$) to less than one-tenth ($m=1600$) of the level attainable without virus. There was a concomitant decrease of the starting time of population collapse from about 28 d ($m=100$) to only 4 d ($m=1600$).

In the LSE experiment used for model calibration (Figure 2), the collapse of the cyanobacteria was followed up by exponential growth of eukaryotic algae, namely green algae. In some of the previous experiments, however, the cyanobacteria did recover after mass lytic events. The simulations showed that—mathematically speaking—the cyanobacterial population would always recover from the first viral outbreak. Even for $m=1600$ the simulations showed a second cycle of growth and collapse after the population density, and thus the probability of collision with viral particles, had become so low as to allow recovery. The next oscillation was so strong that the cyanobacteria became virtually extinct. Increasing amplitude of oscillations also resulted for $m=800$, whereby the cyanobacteria would be extinct after a third cycle of growth and collapse (results not shown).

Expanding the time scale of the simulations to nearly a year (Figure 4) showed increasing oscillations for $m=400$, which eventually might have resulted in virtual extinction as for higher m values. For values of $m=200$ the simulations showed dampening oscillations leading to steady biomass levels. As m was lowered, the steady state was reached earlier and the population density was higher. The viral abundance—not shown in Figure 4 for the sake of clarity—exhibited similar oscillations as the cyanobacteria, but of course the phase was shifted (cf. Figure 2). The steady-state viral abundance was inversely proportional to the cyanobacterial biomass, which is also known from previous experimental work and modelling (e.g. Bratbak et al., 1998). The steady-state numerical virus to host ratios were 2.5, 18 and 60 for $m=50$, 100 and 200, respectively. In these steady states the numbers of infected cells were very small. The greatest share of the infected cells in the total population was for $m=200$, and was still $< 1\%$.

DISCUSSION

It has been well established in experimental as well as model approaches that enlarged burst size decreases both time of the lytic cycle and host population density. The precise impact depends on the specific environment (Levin et al., 1977). Adequate simulation of the cyanobacterial population dynamics in LSE (Figure 2) could be achieved by the modelled feedback between growth and underwater light. Computed values of K_d and μ varied from 4.5 to 6.8 m^{-1} and from 0.30 to 0.21 d^{-1} between time zero and the time of the population peak, respectively. This feedback is important in eutrophic water bodies in general, and very strong in the particular case of hypereutrophic, shallow lakes. Whereas the model fit to cyanobacterial cell numbers was quite good, the computed peak viral abundance in the model calibration (Figure 2) was three to four times as high as the highest virus-like particle (VLP) number observed in LSE experiments (Gons et al., 2002). Part of the discrepancy may be explained by missing the VLP peak in the LSE sampling, but it may also be surmised that a considerable share of the virions in LSE occurred, not free in suspension, but adsorbed onto other particles than cyanobacterial cells. This potential role of the detritus particles in natural water (Barnet et al., 1984; Suttle & Chen, 1992) has not been taken into account in the present model. In fact, other potentially important mechanisms were not considered. Important in both LSE and the original lake water may have been removal of the virions after adsorption onto heterotrophic bacteria or by grazing nanoflagellates. The short bacterial peak observed after that of the VLP in LSE (Gons et al., 2002) indicates the relevance of interactions with other microbiota as in theoretical work (Murray, 1995). Important in the lake may have been viral decay by UV radiation, but not in LSE, since the UV bands lacked in the light source used.

For simulating cyanobacteria–cyanophage interaction in the specific environment of a shallow lake, the present model may be regarded as extremely simple. Nevertheless, the model already requires six coefficients describing the host–virus interaction alone (Table 1). In the specific case described in this article their values were not precisely known, and taken from literature data and incomplete observations made on the LSEs. Even less knowledge exists about their natural variability. For real ecosystems it will certainly not be true that these coefficients remain constant over long periods as in the simulations. Burst size can be expected to vary not only with host species but also to be affected by the hosts' growth rate and nutrient status, see also Parada et al. (2006). Indeed, calculations based on electron micrographs of cyanobacterial cells from Lake Loosdrecht and LSE experiments indicated that m varies by a factor of 100 rather than 10 (M. Tjids, unpublished results). The other important factor determining production of virions is time of the lytic cycle, which like the burst size may vary greatly depending on growth limiting factors (Wilson et al., 1996). These potential variations and their consequences for the cyanobacteria–cyanophage relationship in natural systems merit more study before model predictions can be used with confidence to interpret field observations.

Despite the uncertainties about both viral decay and production, the model results indicate why the apparent

stability of the cyanobacterium–cyanophage relationship in the natural system may be lost in LSE. An important result of the long model runs is the establishment of steady state for relatively small burst sizes. Apparently the stable co-existence of host and virus in this system does not require an additional mechanism such as the phenotypic development of resistance to viral infection (Thyrhaug et al., 2003). Perhaps the question should be reversed. By which factors may stable co-existence, from an evolutionary point of view the preferred outcome for both virus and host in single host–single virus systems, turn into mass killing of the host with potential extinction of both host and virus? The population collapse in LSE has been puzzling in two respects. First, the collapse involved several species of filamentous cyanobacteria. For the present discussion it is surmised that cyanophages attacking the predominating *Limnothrix* sp. may also infect and lyse other species of filamentous cyanobacteria including the prochlorophyte *Prochlorothrix hollandica*. Broad host range of cyanophages has been suspected in early studies, and its existence was demonstrated beyond doubt in recent work on phages associated with marine coccoid cyanobacteria (Sullivan et al., 2003; Millard & Mann, 2006). Second, because the LSE had been specifically designed to maintain the ecosystem structure rather than isolate components thereof (Rijkeboer et al., 1990), it was not understood as to whether a factor stabilizing the cyanobacterium–cyanophage was lost by bringing the lake water into LSE or that the destabilization was specific to physical or chemical conditions in LSE.

The first clue appeared from LSE of Lake Loosdrecht water in which the growth was kept or brought under phosphorus limitation. In these experiments the biomass showed a gradual decline due to the nutrient starvation, but the cyanobacteria recovered as soon as phosphate supply was resumed. In contrast, similarly as shown in Figure 2, the cyanobacterial population collapsed in the 'control' LSE with high phosphate supply from the onset of the experiment (Gons et al., 2002). These observations combined with the modelled effect of burst size indicates that a transition from phosphorus-limited growth, as in the lake in summer, to light-limited growth, as experimentally imposed to the LSE, is a key factor leading to population collapse. This impact of nutrient status conforms to the concept of density-dependence of parasites within hosts in a general theory on host–pathogen interaction. In the lake, the cyanobacteria and cyanophages will be able to co-exist owing to relatively small burst size due to phosphorus limitation. High external nutrient loading will not only speed up the cyanobacterial growth but also involve rapid increase in burst size as enabled by enhanced nucleotide content of the host (Brown et al., 2006). If the viral decay rate cannot match the increased production of virions, the cyanobacterial population will inevitably collapse.

As previously noted, unequivocal demonstration of virally-induced collapse of natural cyanobacterial populations is still lacking. Circumstantial evidence includes the vanishing of *Planktothrix agardhii* in the shallow Lake Tjeukemeer (The Netherlands) in 1985 (Gons et al., 2002). It is tempting to also attribute to cyanophagy the cyanobacterial collapse following experimental whole-lake phosphorus loading in the Canadian Experimental

Lake Area (Schindler, 1974). Although not improbable (D.W. Schindler, personal communication) such a past impact of cyanophages cannot be ascertained. Dedicated observations on mass lytic events made with current methods of preservation and enumeration are awaited.

Thanks are due to Dr M. Heldal (Department of Microbiology, University of Bergen, Norway), and to Dr J.H. Janse (Netherlands Environmental Assessment Agency, Bilthoven, The Netherlands) for their kind help with electron microscopy, and discussion of model aspects, respectively. The contribution of S.G.H. Simis was funded by grant EO-053 from the User Support Programme managed by the programme office External Research of the Netherlands Organization for Scientific Research (NWO)—National Institute for Space Research (SRON). The contribution of M. Tjldens was funded by grant 809.34.006 from the NWO sector of Earth and Life Sciences (ALW). Publication 3811 NIOO-KNAW Netherlands Institute of Ecology, Centre for Limnology.

REFERENCES

- Barnet, Y.M., Daft, M.J. & Stewart, W.D.P., 1984. The effect of suspended particulate material on cyanobacteria–cyanophage interactions in liquid culture. *Journal of Applied Bacteriology*, **56**, 109–115.
- Bratbak, G., Jacobsen, A., Heldal, M., Nagasaki, K. & Thingstad, F., 1998. Virus production in *Phaeocystis pouchetii* and its relation to host cell growth and nutrition. *Aquatic Microbial Ecology*, **16**, 1–9.
- Brown, C.M., Lawrence, J.E. & Campbell, D.A., 2006. Are phytoplankton population density maxima predictable through analysis of host and viral genomic DNA content? *Journal of the Marine Biological Association of the United Kingdom*, **86**, 491–498.
- Gons, H.J., 1995. Interaction of detritus with abundance of cyanobacteria and microalgae. *Water Science and Technology*, **32**, 129–138.
- Gons, H.J., Ebert, J., Hoogveld, H.L., Van den Hove, L., Pel, R., Takkenberg, W. & Woldringh, C.J., 2002. Observations on cyanobacterial population collapse in eutrophic lake water. *Antonie van Leeuwenhoek*, **81**, 319–326.
- Levin, B.R., Stewart, F.M. & Chao, L., 1977. Resource-limited growth, competition, and predation: a model and experimental studies with bacteria and bacteriophage. *American Naturalist*, **111**, 3–24.
- Millard, A.D. & Mann, N.H., 2006. A temporal and spatial investigation of cyanophage abundance in the Gulf of Aqaba, Red Sea. *Journal of the Marine Biological Association of the United Kingdom*, **86**, 507–515.
- Mühling, M. et al., 2005. Genetic diversity of marine *Synechococcus* and co-occurring cyanophage communities: evidence for viral control of phytoplankton. *Environmental Microbiology*, **7**, 499–508.
- Murray, A.G., 1995. Phytoplankton exudation: exploitation of the microbial loop as a defence against algal viruses. *Journal of Plankton Research*, **17**, 1079–1094.
- Murray, A.G. & Jackson, G.A., 1992. Viral dynamics: a model of the effects of size, shape, motion and abundance of single-celled planktonic organisms and other particles. *Marine Ecological Progress Series*, **89**, 103–116.
- Neale, P.J., Talling, J.F., Heaney, S.I., Reynolds, C.S. & Lund, J.W.G., 1991. Long time series from the English Lake District: irradiance-dependent phytoplankton dynamics during the spring maximum. *Limnology and Oceanography*, **36**, 751–760.
- Padan, E., Ginzburg, D. & Shilo, M., 1970. The reproductive cycle of cyanophage LPP1-G in *Plectonema boryanum* and its dependence on photosynthetic and respiratory system. *Virology*, **40**, 514–521.
- Padan, E. & Shilo, M., 1969a. Distribution of cyanophages in natural habitats. *Proceedings of the Congress of the International Association of Theoretical and Applied Limnology*, **17**, 747–751. [Stuttgart: Schweizerbart.]
- Padan, E. & Shilo, M., 1969b. Short trichome mutant of *Plectonema boryanum*. *Journal of Bacteriology*, **97**, 975–976.
- Parada, V., Herndl, G.J. & Weinbauer, M.G., 2006. Viral burst size of prokaryotes in aquatic systems. *Journal of the Marine Biological Association of the United Kingdom*, **86**, 613–612.
- Rijkeboer, M., De Bles, F. & Gons, H.J., 1990. Laboratory scale enclosure: concept, construction and operation. *Journal of Plankton Research*, **12**, 231–244.
- Rijkeboer, M., Gons, H.J. & Kromkamp, J., 1993. Preservation of the light field in turbid lake and river water in laboratory-scale enclosure. *Journal of Plankton Research*, **15**, 517–530.
- Schindler, D.W., 1974. Eutrophication and recovery in experimental lakes: implications for lake management. *Science, New York*, **184**, 897–899.
- Sherman, L.A. & Haselkorn, R., 1971. Growth of the blue-green algae virus LPP-1 under conditions which impair photosynthesis. *Virology*, **45**, 739–746.
- Simis, S.G.H., Tjldens, M., Hoogveld, H.L. & Gons, H.J., 2005. Optical changes associated with cyanobacterial bloom termination by viral lysis. *Journal of Plankton Research*, **27**, 937–949.
- Sullivan, M.B., Waterbury, J.B. & Chisholm, S.W., 2003. Cyanophages infecting the oceanic cyanobacterium *Prochlorococcus*. *Nature, London*, **424**, 1047–1051.
- Suttle, C.A., 2000. Cyanophages and their role in the ecology of cyanobacteria. In *The ecology of cyanobacteria* (ed. B.A. Whitton and M. Potts), pp. 563–589. Dordrecht: Kluwer Academic Publishers.
- Suttle, C.A., 2005. Viruses in the sea. *Nature, London*, **437**, 356–361.
- Suttle, C.A. & Chan, A.M., 1993. Marine cyanophages infecting oceanic and coastal strains of *Synechococcus*: abundance, morphology, cross-infectivity and growth characteristics. *Marine Ecology Progress Series*, **92**, 99–109.
- Suttle, C.A. & Chen, F., 1992. Mechanisms and rates of decay of marine virus in seawater. *Applied and Environmental Microbiology*, **58**, 3721–3729.
- Thingstad, T.F. & Lignell, R., 1997. A theoretical approach to the question of how trophic interactions control carbon demand, growth rate, abundance, and diversity. *Aquatic Microbial Ecology*, **13**, 19–27.
- Thyrhaug, R., Larsen, A., Thingstad, F. & Bratbak, G., 2003. Stable coexistence in marine algal host–virus systems. *Marine Ecology Progress Series*, **254**, 27–35.
- Van Hanne, E.J., Zwart, G., Van Agterveld, M.P., Gons, H.J., Ebert, J. & Laanbroek, H.J., 1999. Changes in bacterial and eukaryotic community structure after mass lysis of filamentous cyanobacteria associated with viruses. *Applied and Environmental Microbiology*, **65**, 795–801.
- Van Tongeren, O.F.R., Van Liere, L., Gulati, R.D., Postema, G. & Boesewinkel-de Bruyn, P.J., 1992. Multivariate analyses of the plankton communities in the Loosdrecht lakes: relationship with the chemical and physical environment. *Hydrobiologia*, **233**, 105–117.
- Wilson, W.H., Carr, N.G. & Mann, N.H., 1996. The effect of phosphate status on the kinetics of cyanophage infection in the oceanic cyanobacterium *Synechococcus* sp. WH7803. *Journal of Phycology*, **32**, 506–516.
- Wommack, K.E. & Colwell, R.R., 2000. Virioplankton: viruses in aquatic ecosystems. *Microbiology and Molecular Biology Reviews*, **64**, 69–114.
- Zwart, G., Kamst-van Agterveld, M.P., Van der Werff-Staverman, I., Hagen, F., Hoogveld, H.L. & Gons, H.J., 2005. Molecular characterization of cyanobacterial diversity in a shallow eutrophic lake. *Environmental Microbiology*, **7**, 365–377.

Submitted 21 December 2005. Accepted 22 March 2006.